

A Comparison of Signal-to-Noise Characteristics: Fourier Transform Enhanced Magnetic  
Rotation Spectroscopy and Dispersive Spectrometry.

by

Neme O. Nnolim

B.S., Chemical Engineering  
University of Rochester, 1992

Submitted to the Department of Chemistry  
in Partial Fulfillment of the Requirements for the Degree of

MASTER OF SCIENCE  
in Physical Chemistry  
at the

Massachusetts Institute of Technology

September 1995

© 1995 Neme O. Nnolim

All rights reserved

The Author hereby grants to MIT permission to reproduce and to distribute publicly paper and  
electronic copies of this thesis document in whole or in part.

Signature of Author .....

Department of Chemistry  
September 1, 1995

Certified by .....

Accepted by .....

MASSACHUSETTS INSTITUTE  
OF TECHNOLOGY

SEP 12 1995

LIBRARIES

Science

## TABLE OF CONTENTS

	PAGE
Abstract.	3
The Fourier Transform spectrometer.	4
Optical throughput and resolution.	10
Magnetic rotation spectroscopy.	13
The signal-to-noise ratio of detection.	16
Derivation of signal-to-noise ratio expressions.	17
Calculation of signal-to-noise ratios for the ${}^2\Pi_{1/2}$ , P(3/2) line in the $A^2\Sigma^+ - X^2\Pi$ transition of OH.	21
References.	26

A Comparison of Signal-to-Noise Characteristics:  
Fourier Transform enhanced Magnetic Rotation Spectroscopy and Dispersive Spectrometry

by

Neme O. Nnolim

Submitted to the Department of Chemistry on September 1, 1995  
in Partial Fulfillment of the Requirements for the Degree of  
Master of Science in Physical Chemistry

ABSTRACT

Using the same source irradiance, calculations are done for the magnitude of the signal-to-noise ratio of detection for the P(3/2) absorption line of the OH radical using a grating spectrometer and a Fourier Transform (FT) spectrometer. For the same source irradiance, the optical throughput of a FT spectrometer at any given resolution is greater than that of a grating spectrometer. This is especially advantageous when weak sources must be used. The noise in the FT spectrum is spread around the spectrum so that when the source is monochromatic, the signal-to-noise ratio about a single line is enhanced. This advantage vanishes when a continuous, broad-band source is used.

The time taken to record a spectrum at a given signal-to-noise ratio is less for the FT spectrometer by a factor equal to the number of spectral resolution elements. Conversely, for a given total recording time, the time spent on a spectral resolution element using a FT spectrometer to record a spectrum is greater than the time spent on a resolution element using a grating spectrograph by a factor equal to the square root of the number of resolution elements in the spectrum. This is known as the multiplex advantage of the FT spectrometer. The signal-to-noise ratio of detection is proportional to the square root of the time of detection, so that this advantage can result in improved signal-to-noise ratio but only when the dominant form of noise in the experiment is detector noise. However, due to the fact that the noise from the photomultiplier detectors used in the UV region is proportional to the square root of the signal strength, the dominant form of noise in this region is shot noise.

Using the MRS technique with the optimum uncrossing angle between nearly crossed polarizers, the magnitude of the experimental shot noise is shown to be reduced to below that of the detector noise so that in this instance the multiplex advantage of the Fourier Transform spectrometer will result in improved signal-to-noise ratio when it is coupled with the MRS technique for the detection of this absorption line. The signal-to-noise ratio using the FT spectrometer can also be improved by averaging over a large number of scans; but then the improvement in signal-to-noise ratio is limited by the memory capacity of the computer used to process the spectral data. This is especially so if the initial signal-to-noise ratio is large.

Thesis Supervisor: Robert Field

Title: Professor of Chemistry

## THE FOURIER TRANSFORM SPECTROMETER

The Michelson interferometer is the basic unit of the Fourier transform spectrometer. The interferometer generates two waves of equal amplitude from an incoming wave by division at a beamsplitter, and introduces a phase shift into one of the waves. The two beams are recombined at the beamsplitter after reflection from two mirrors, one moving and one stationary. The beams will then interfere constructively or destructively depending on the path difference between them. The path difference between the two beams is introduced by the moving mirror arm of the interferometer which changes the path length travelled by one of the beams relative to the other.

This can be seen by considering two waves of the same amplitude,

$$\psi_1 = A\cos(2\pi x_1 \bar{\nu}) \text{ and } \psi_2 = A\cos(2\pi x_2 \bar{\nu}). \quad (1)$$

which can be added to obtain a resultant wave of the same frequency as each of the original waves, but phase shifted by an amount  $\delta/2$  where  $x_1 - x_2 = \delta$  and  $x_2 = x$

$$\psi = \psi_1 + \psi_2. \quad (2)$$

$$= A[\cos(2\pi x_1 \bar{\nu}) + \cos(2\pi x_2 \bar{\nu})]. \quad (3)$$

$$= 2A\cos[\pi \bar{\nu}(x_1 - x_2)]\cos[\pi \bar{\nu}(x_1 + x_2)]. \quad (4)$$

$$\psi = 2A\cos(\pi \bar{\nu} \delta)\cos[2\pi \bar{\nu}(x + \delta/2)]. \quad (5)$$

The amplitude can vary between  $2A$  and zero. The square of the amplitude, the intensity, is the measurable quantity.

$$\text{The amplitude, } A_\psi = 2A\cos(\pi \bar{\nu} \delta). \quad (6)$$

The intensity  $I = A_\psi^2 = 4A^2\cos^2(\pi \bar{\nu} \delta)$ . Since  $A^2$  is the incident intensity ( $I_0$ ) of each wave,

$$I = 4I_0\cos^2(\pi \bar{\nu} \delta) = 2I_0[1 + \cos(2\pi \bar{\nu} \delta)]. \quad (7)$$

The intensity  $I$  will alternate between  $4I_0$  and 0 as the pathlength difference changes through a wavelength. Two waves having a fixed phase relationship are necessary for two beam interference to occur in this way. If a detector is used to detect the interference pattern, the detector output will alternate between a maximum corresponding to the incoming intensity and zero when the path difference changes such that there is a phase change through  $\pi$  radians. The light not reaching the detector will return to the source.

In the Michelson interferometer, one arm moves at a constant velocity of  $V$  cm/s. When illuminated by a monochromatic point source, the detector will see a periodically varying signal.

The rate of change of path difference  $d\Delta/dt = 2V$  cm/s so that the electrical frequency  $f$  of the

wave is equal to  $2\bar{\nu}V$  Hertz.

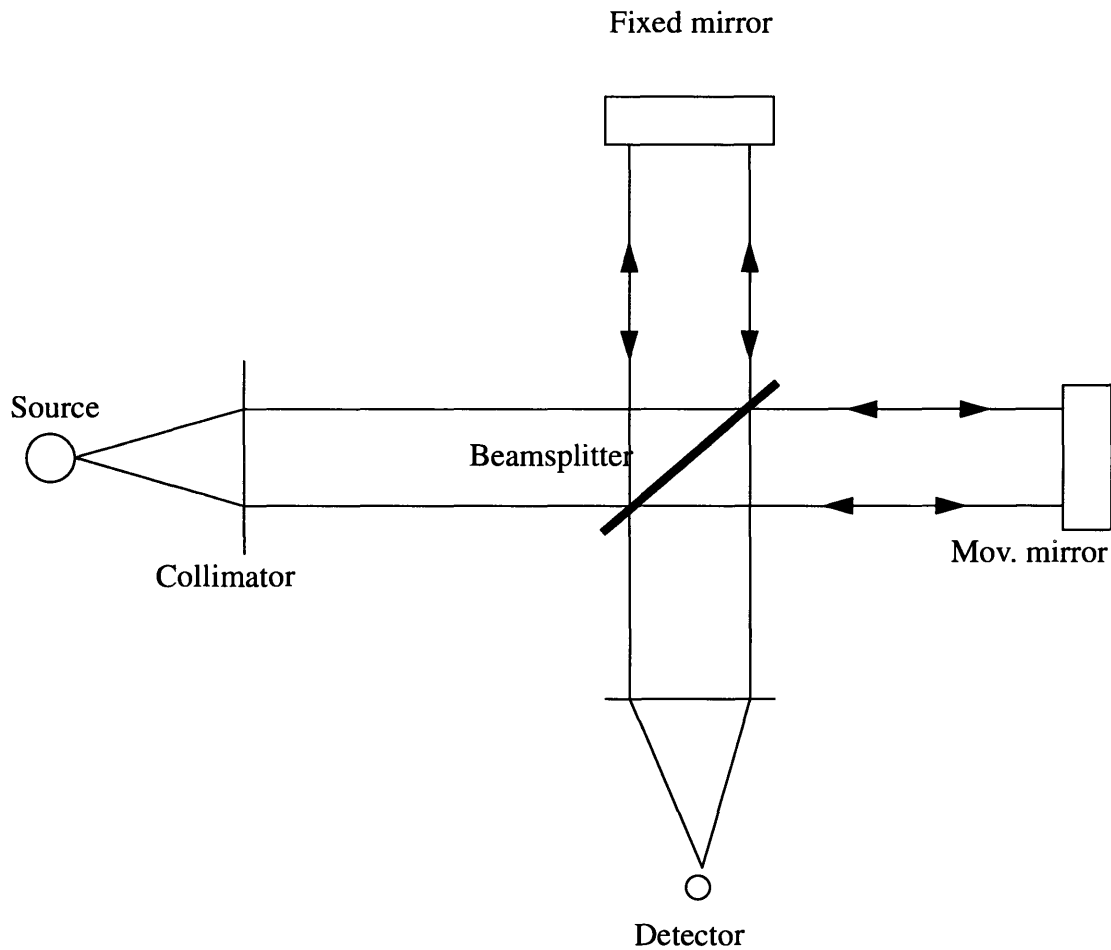


Fig.1: The Michelson interferometer

If the monochromatic source is replaced with a broad-band source which contains a range of optical frequencies, the different frequencies in the broad-band source are independently transformed into a range of electrical frequencies. The Fourier transform is used to measure the amplitudes of each of the electrical frequencies.

If  $2I_0$  is replaced by  $S$  (incoming monochromatic intensity),

$$\text{then } I(x) = S[1 + \cos(2\pi\bar{\nu}x)]. \tag{8}$$

where the path difference  $\delta$  has been changed to  $x$ .

Replacing the monochromatic source by a broadband source requires replacing  $S$  by  $S(\bar{\nu})$  and integrating over frequency:

$$\begin{aligned}
I(x) &= \int_{-\infty}^{\infty} S(\bar{\nu}) [1 + \cos(2\pi\bar{\nu}x)] d\bar{\nu}. \\
&= \int_{-\infty}^{\infty} S(\bar{\nu}) d\bar{\nu} + \int_{-\infty}^{\infty} S(\bar{\nu}) \cos(2\pi\bar{\nu}x) d\bar{\nu}.
\end{aligned} \tag{9}$$

The first term in Eq.(9) is the total incident energy which is constant and can be subtracted from  $I(x)$ .

The second modulated part of Eq.(9) contains all the useful spectral information.

Two functions  $s(x)$  and  $S(\bar{\nu})$  are said to be a Fourier transform pair if

$$\begin{aligned}
s(x) &= 1/2\pi \int_{-\infty}^{\infty} S(\bar{\nu}) e^{2\pi i\bar{\nu}x} d\bar{\nu} \quad \text{and} \\
S(\bar{\nu}) &= 1/2\pi \int_{-\infty}^{\infty} s(x) e^{-2\pi i\bar{\nu}x} dx.
\end{aligned} \tag{10}$$

In this case,  $s(x)$  is the Fourier transform of  $S(\bar{\nu})$ , and  $S(\bar{\nu})$  is the inverse Fourier transform of  $s(x)$ .

$$\begin{aligned}
s(x) &= 1/2\pi \int_{-\infty}^{\infty} S(\bar{\nu}) e^{2\pi i\bar{\nu}x} d\bar{\nu} = 1/2\pi \int_{-\infty}^{\infty} S(\bar{\nu}) [\cos(2\pi\bar{\nu}x) + i\sin(2\pi\bar{\nu}x)] d\bar{\nu}. \\
&= 1/2\pi \int_{-\infty}^{\infty} S(\bar{\nu}) \cos(2\pi\bar{\nu}x) d\bar{\nu} \quad \text{if the imaginary part is discarded.}
\end{aligned} \tag{11}$$

Eq. (11) is the cosine Fourier transform of  $S(\bar{\nu})$ .

The modulated part of  $I(x)$  is therefore equal to the cosine Fourier transform of  $S(\bar{\nu})$  because the observed spectrum is real.

In practice,  $x$  is measured at discrete intervals by the interferometer so the integral has to be replaced by a summation and the interferogram can be generated only over a finite range of path difference which means that  $s(x)$  is multiplied by a boxcar function  $b(x)$  which takes the value 1 between  $x=0$  and  $x = L$  ( $L =$  maximum path difference) and 0 everywhere else.

$$S(\bar{\nu}) \text{ is then modified to } S'(\bar{\nu}) = \int_{-\infty}^{\infty} s(x)b(x)\cos(2\pi\bar{\nu}x)dx. \tag{12}$$

where  $b(x) = 1$  for  $0 \leq x \leq L$  and 0 everywhere else.  $S(\bar{\nu})$ , the desired spectrum, is related to  $S'(\bar{\nu})$ , the spectrum which is actually obtained from the FT spectrometer, by a convolution.

The convolution  $f(t)$  of two functions  $g(t)$  and  $h(t)$  is defined as,

$$f(t) = \int_{-\infty}^{\infty} g(t)h(t)e^{-2\pi i vt} dt = \int_{-\infty}^{\infty} G(v')H(v - v')dv' . \quad (13)$$

If  $F(\bar{v})$ ,  $G(\bar{v})$  and  $H(\bar{v})$  represent the Fourier transforms of the functions  $f(t)$ ,  $g(t)$  and  $h(t)$  respectively,

$$\text{then } F(\bar{v}) = G(\bar{v})H(\bar{v}). \quad (14)$$

The relationship between  $S(\bar{v})$  and  $S'(\bar{v})$  is therefore,

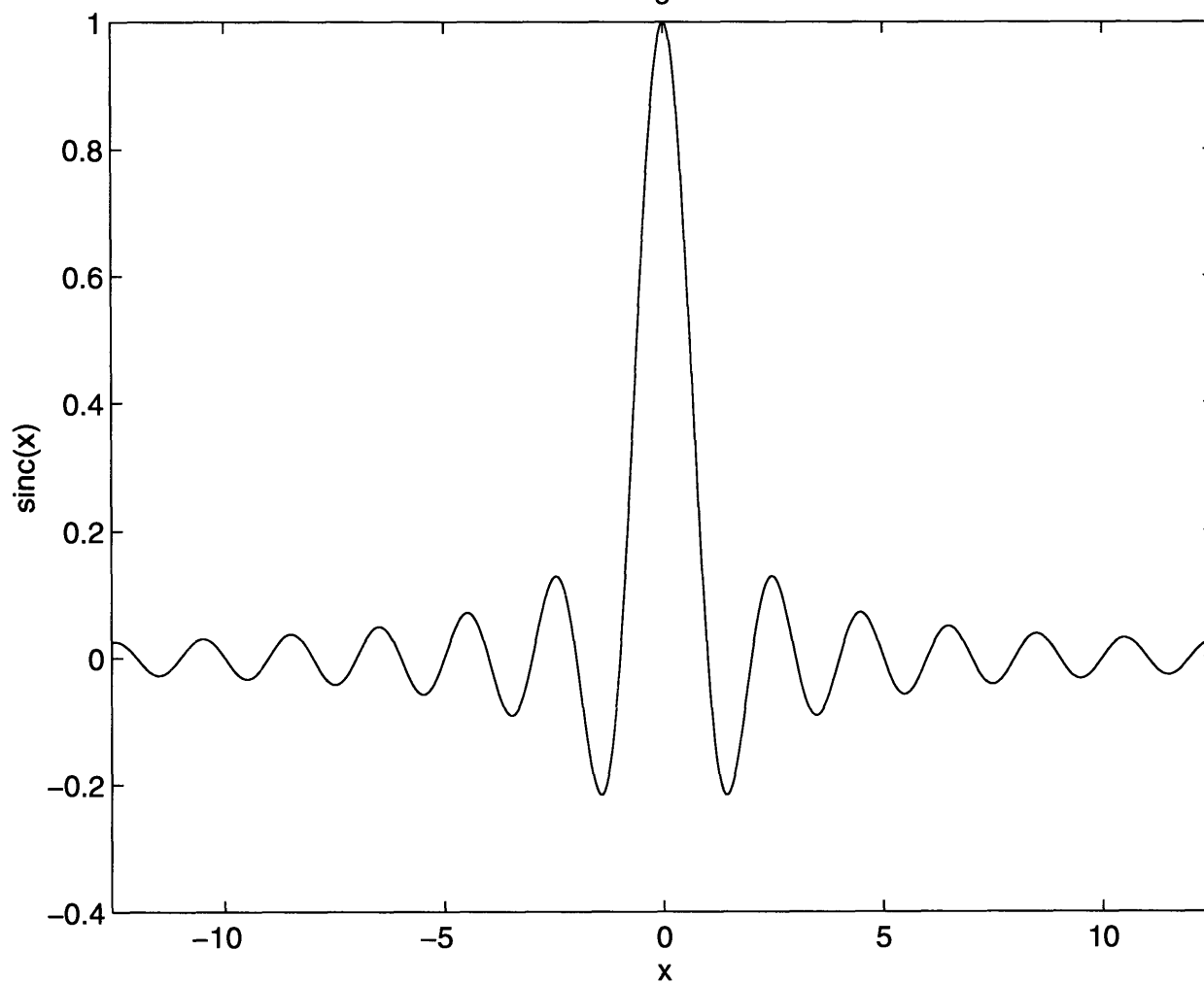
$$S'(\bar{v}) = S(\bar{v})B(\bar{v}), \quad (15)$$

where  $B(\bar{v})$  is the Fourier transform of the boxcar function  $b(x)$ .

$$\text{With normalization, } B(\bar{v}) = \sin(2\pi\bar{v}L)/(2\pi\bar{v}L) \quad (16)$$

=  $\text{sinc}(2\pi\bar{v}L)$  where  $L$  is the maximum pathlength of the moving mirror in cm.

Fig.2

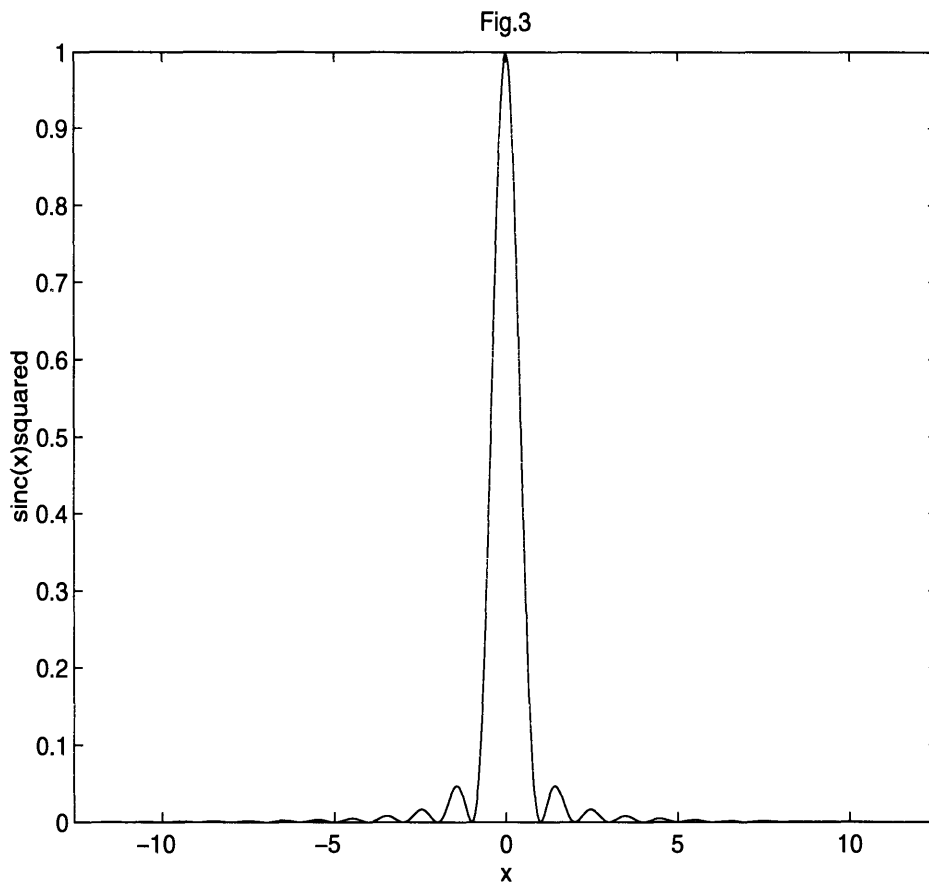


The Instrument Function (IF) is the response of the FT spectrometer when it measures radiation at a frequency  $\bar{\nu}$ . It is used to define the resolution of a spectrometer quantitatively.

Two narrow lines of the same intensity are said to be resolved by the baseline criterion when the separation between the lines is such that any further reduction in the separation will result in the reduction of the depth of the valley between the lines to less than 100% of the line intensities.

The two lines are said to be resolved by the Rayleigh criterion when the separation between the lines is such that the depth of the valley between the lines is not less than 20% of the intensity of the lines. As shown above, the Fourier transform of the boxcar function is a sinc function. This function (Fig.2) has side-peaks on either side of the main peak which decrease in amplitude as the distance from the center of the main peak increases in either direction. These side-peaks decrease the signal-to-noise ratio of detection because a spectral line with a linewidth comparable to that of one of the side-peaks of a strong line will not be distinguishable as a spectral line. To remove the side-peaks, an apodizing function is convolved with the spectrum  $S(\bar{\nu})$ . The most common apodizing function is a triangular function of the form  $f_A(x) = 1 - |x|/L$ . The Fourier transform of this function is  $\text{sinc}^2(\pi L \bar{\nu})$  which is the Instrumental Function (IF) in this case.





In the previous case of no apodization, the IF is  $\text{sinc}(2\pi\sqrt{L})$ , the FT of the boxcar function.

The resolution of an FTS is conventionally defined as the FWHM of the main peak of the IF. The FWHM of the sinc IF for a maximum pathlength of  $L$  is  $0.604/L$  and the width of the baseline of the main peak is  $1/L$ . The FWHM of the  $\text{sinc}^2$  IF for the same maximum pathlength is  $0.88/L$  and the width of the baseline of the main peak is  $2/L$ . The  $\text{sinc}^2$  function (Fig.3) has a baseline width twice that of the sinc function so that the moving mirror in the FT spectrometer has to move twice the distance it would have to move if the interferogram were not apodized to achieve the same resolution. Thus the resolution of the instrument has been reduced by a factor of 2 due to apodization while the signal-to-noise ratio has improved because the spectrum is being convolved with an IF with much smaller side peaks.

## OPTICAL THROUGHPUT AND RESOLUTION

One of the major factors affecting the signal-to-noise ratio (S/N) in an optical system is the product of the area  $A$  of the light beam going through the system and the solid angle  $\Omega$  contained within the beam. This is the *etendue* of the system. The critical factor for a dispersive spectrometer is usually the prism or grating in the spectrometer. The beamsplitter is usually the critical factor in a FT spectrometer.

Light containing a finite range of angles goes through the interferometer because of the finite size of real sources. For example, if the source is circular with radius  $a$ , and the collimator focal length is  $f$ , the range of angles going through the system is  $a/f$  radians.

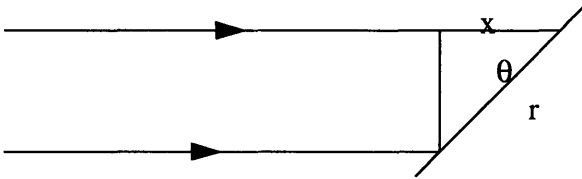


Fig.4: Light incident on a beamsplitter

Fig.4 shows a beam of light incident on a beamsplitter of length  $r$  exposed to the beam. The path difference,  $x$ , between the extreme rays of the light beam is  $r\cos\theta$ .

The path difference must be made up of an integral number,  $n$ , of half-wavelengths for constructive interference so that,

$$n\lambda = 2r\cos\theta. \quad (17)$$

If the interferometer is in a medium of refractive index  $\chi$ ,  $\lambda$  is reduced so that,

$$n\lambda = 2\chi r\cos\theta. \quad (18)$$

$$\text{or } n = 2\chi\bar{v}r\cos\theta. \quad (19)$$

These expressions illustrate the relation between the solid angle contained by the incoming light and spectral resolution, as will be shown below.

For a light ray of wavelength  $\lambda_0$  close to and parallel to the center axis of the light beam,

$$n\lambda_0 = 2\chi r. \quad (20)$$

A light ray contained in the beam which is farther away from the center axis of the beam will make a small angle of  $\theta$  with the axis due to divergence.

For a light ray of wavelength  $\lambda_1$  at an angle  $\theta$  to the center axis of the beam,

$$n\lambda_1 = 2\chi r\cos\theta \cong 2\chi r (1 - \theta^2/2), \quad (21)$$

where the same integer number,  $n$ , of wavelengths is required.

Letting  $\lambda_0 - \lambda_1 = \delta\lambda$  and  $\lambda_0 = \lambda$ ,

$$\delta\lambda/\lambda = \theta^2/2 = \delta\bar{v}/\bar{v}, \quad (22)$$

where  $\theta$  is the halfangle of the solid angle cone subtending  $\Omega$  steradians.

$$\Omega = \pi\theta^2. \quad (23)$$

$$\delta\lambda/\lambda = \delta\bar{v}/\bar{v} = \Omega/2\pi. \quad (24)$$

This expression relates the solid angle contained by the light going through the FTS to the spectral resolution attainable with the instrument.

The throughput is the product of the *etendue* with the overall system transmittance,  $\tau$ . Diffraction grating spectrometers generally provide greater throughput than prism grating spectrometers, so diffraction grating spectrometers will be used for comparison to the FT spectrometer.

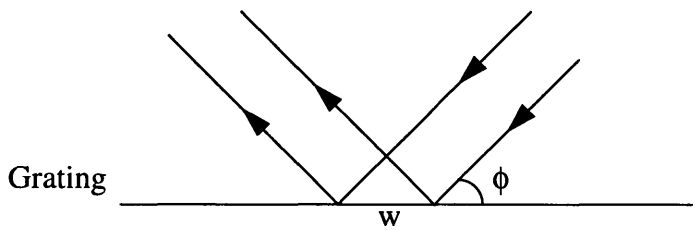


Fig.5 The grating as a dispersing instrument

The width  $w$  between rulings on a diffraction grating is given by,

$$w = n\lambda/2\sin\phi. \quad (25)$$

where  $n$  is the order of diffraction and  $\phi$  is the blaze angle of the grating.

The closer to its blaze angle a grating is used, the more efficient it will be in dispersing radiation.

The angular dispersion of the grating is,

$$\delta\phi = n\delta\lambda/2w\cos\phi = \tan\phi\delta\lambda/\lambda. \quad (26)$$

$$\Omega = \delta\phi\beta = \beta\tan\phi\delta\lambda/\lambda. \quad (27)$$

where  $\beta$  is the angle in radians subtended at the grating by the entrance slit-width of the grating spectrometer.

If  $S$  is the area of the grating, The area  $A$  of the light beam is  $A = S\cos\phi$ .

$$\text{so } (A\Omega)_{\text{grating}} = S\beta\sin\phi (\delta\lambda/\lambda). \quad (28)$$

For the same light beam cross-sectional area and spectral resolution in the FT and grating spectrograph,,

$$(A\Omega)_{\text{FTS}}/(A\Omega)_{\text{grating}} = \sqrt{2} \pi/\beta \sin\phi. \quad (29)$$

$\sin\phi$  can take on a maximum (unlikely) value of 1.  $\beta$  is unlikely to be greater than 0.033 therefore a FT instrument in which the moving mirror can move a maximum displacement  $L$  has an advantage of a factor of about 150 in terms of optical throughput over a grating instrument of length  $L$ .

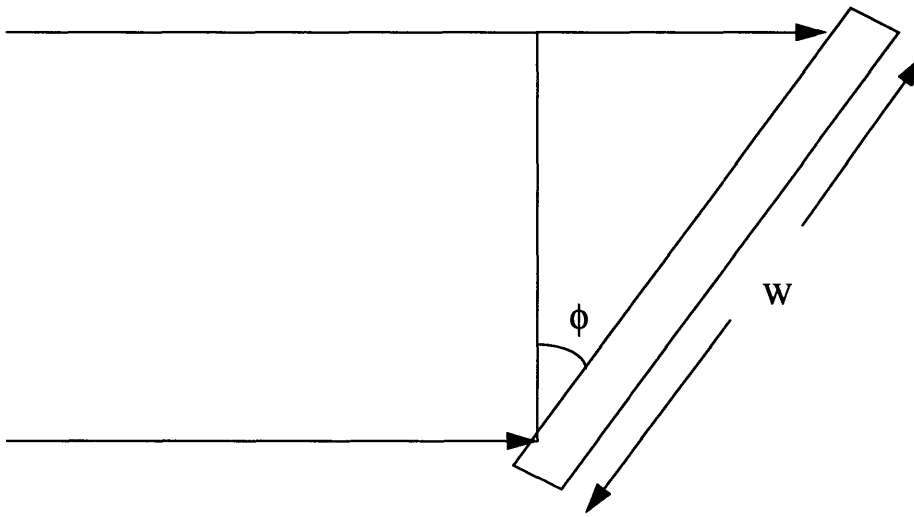


Fig. 6 : Light incident on a grating of length  $W$

For a grating of length  $W$  and blaze angle  $\phi$ , the difference in the paths travelled by the extreme rays of the light beam is  $W \sin\phi$ .

At any wavelength  $\lambda$ , the path difference is made up of an integral number of wavelengths  $k$ .

$$k\lambda = W \sin\phi. \quad (30)$$

Resolution of a wavelength  $(\lambda + \delta\lambda)$  occurs when,

$$(k - 1/2)(\lambda + \delta\lambda) = W \sin\phi. \quad (31)$$

substituting for  $k$ , and neglecting the small term  $\delta\lambda/2$ ,

$$\delta\lambda/\lambda \cong \lambda/(2W \sin\phi). \quad (32)$$

$$\delta\lambda/\lambda = \delta\bar{\nu}/\bar{\nu} \text{ and } \bar{\nu}\lambda = 1. \quad (33)$$

$$\text{so } \delta\bar{\nu} = 1/(2W\sin\phi). \quad (34)$$

This shows that the resolution attainable with the grating improves as its width  $W$  perpendicular to the ruled grooves is increased. This applies when the grating is used at its limit of resolution. But this is rarely possible. Usually the widths of the entrance and exit apertures of the spectrometer are used to determine the resolution.

### MAGNETIC ROTATION SPECTROSCOPY

MRS (Magnetic rotation spectroscopy) operates on the principle that a transition in a paramagnetic molecule can alter the state of polarization of linearly polarized light in the presence of a magnetic field of suitable strength parallel to the direction of propagation of the light.

Linearly polarized light will consist of equal amplitudes of left and right circularly polarized radiation. Application of the field will result in unequal indices of refraction for RCP and LCP light, thereby rotating the plane of polarization. This is the phenomenon of magnetic circular birefringence (MCB). The two polarizations will also have different absorption coefficients as a result of the application of the magnetic field. This is magnetic circular dichroism (MCD).

MRS is a result of these two effects on the RCP and LCP light components as they go through the absorbing medium. The RCP and LCP waves are differentially absorbed and differentially phase shifted.

The signal is detected through a polarizer set at  $90^\circ + \xi$  to the polarization plane of the incident light where  $\xi$  is a small uncrossing angle selected to optimize the signal to noise ratio.

Transitions which do not alter the state of polarization of the incident light will not be detected.

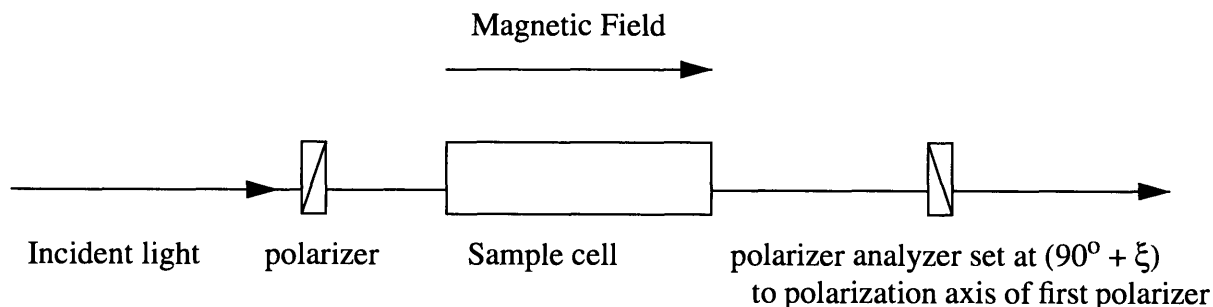


Fig.7: Schematic of MRS technique.

Each transition can be regarded as a collection of doublets with  $\Delta M = +1$  and  $\Delta M = -1$

components split by the Zeeman effect. The MRS signal is a sum of two M- averaged dispersion curves,  $[M = J, J - 1, J - 2, \dots, (J - 1), -J]$  displaced slightly in frequency. An MRS effect will be observed whenever the Zeeman splitting between  $(J, M + 1)$  and  $(J, M - 1)$  levels is larger than the homogeneous linewidth.

The power passed through the polarizer after the sample cell is,

$$P(\xi) = (P_0/2)\exp(-2I_A L)[\cosh(I_\Delta L) - \cos(R_\Delta L + 2\xi)]. \quad (35)$$

where  $P(\xi)$  is the power passed through the polarizer after the sample which is oriented at an angle  $\xi + 90^\circ$  with respect to the incident plane of polarization,  $P_0$  is the power incident on the sample,  $I_A$  is the average attenuation of the fields of the two circular waves,  $L$  is the path length,  $I_\Delta$  is the difference in the attenuation of the fields of the two circular waves (RCP - LCP) and  $R_\Delta$  is the difference in the real parts of the field propagation constants for the two circular polarizations (RCP - LCP). For a weak absorption line and small  $\xi$ , the power passed reduces to,

$$P(\xi) = (P_0/2)(1 - \cos 2\xi). \quad (36)$$

neglecting terms in the square of the propagation constants and assuming that the polarizers will not be crossed exactly.

The signal  $S$  is given by,

$$S = (P_T P_0)^{1/2} R_\Delta L. \quad (37)$$

If the extinction ratio of the polarizer is  $\alpha$ , the optimum signal-to-noise ratio is achieved when the polarizer is deliberately offset so that the total transmitted light is  $2\alpha P_0$ . The signal to transmitted power ratio is given by,

$$S/P = R_\Delta L / (2\alpha)^{1/2}. \quad (38)$$

The sensitivity of detection is defined as the ratio of the signal on resonance to the noise off resonance. The sensitivity in laser based MRS experiments is practically limited by the polarizer extinction ratio,  $\alpha$ .  $\alpha$  is typically  $< 10^{-6}$ . With a greatly improved polarizer, the sensitivity can be limited by detector noise or shot noise. However, there is a limit to the quality of polarizers. If the polarizer is nearly crossed but  $\alpha P_0$  is small compared to  $P_T$ , then as the polarizer is further crossed, the signal decreases as the square root of the transmitted power, the source noise decreases linearly with transmitted power, detector noise is independent of transmitted power, and shot noise decreases as the square root of transmitted power, so that either detector noise or shot noise will limit the ultimate sensitivity of detection.

In MRS, the power from a monochromatic source passed through the polarizer after the sample, for a weak line and small uncrossing angle  $\xi$  is,

$$P_T = P_0(1 - \cos 2\xi)/2. \quad (39)$$

$$\text{The signal is equal to } R_\Delta L \sqrt{P_T P_0}. \quad (40)$$

The maximum reduction in source noise occurs when  $P_T = 2\alpha P_0$  where  $\alpha$  is the extinction coefficient of the polarizer.

Since  $P_T = P_0(1 - \cos 2\xi)/2$ , the optimum uncrossing angle of the polarizer analyzer for maximum signal-to-noise ratio will be given by,

$$\xi_{\text{opt}} = [\cos^{-1}(1 - 4\alpha)]/2. \quad (41)$$

$$\text{The signal can therefore be written as } R_{\Delta} L P_0 \sqrt{2\alpha}. \quad (42)$$

$$\text{where } R_{\Delta} = \sum_{M_J} [R_+(M_J) - R_-(M_J)]. \quad (43)$$

The + and - subscripts denote  $\Delta M_J = +1$  and  $\Delta M_J = -1$  transitions respectively. An expression for the R terms has been derived by Litfin, et al. These are valid for Doppler and Lorentzian line-shapes.

$$R_+(M_J) = \frac{N_i |\langle j | \mu_{ij} | i \rangle|^2}{g_i 2uh\epsilon_0} \text{ReZ}[(\Delta v_+ + i\delta)\lambda/u]. \quad (44)$$

$$R_-(M_J) = \frac{N_i |\langle j | \mu_{ij} | i \rangle|^2}{g_i 2uh\epsilon_0} \text{ReZ}[(\Delta v_- + i\delta)\lambda/u]. \quad (45)$$

where  $\delta$  is the homogeneous (Lorentzian) half width at half maximum of the transition,

$\lambda$  is the light wavelength,

$\epsilon_0$  is the permittivity of free space,

$u$  is the most probable molecular speed,

$N_i$  is the population density of the molecules in the  $i$ th Zeeman level per cubic meter,

$g_i$  is the degeneracy of the energy level,

$|\langle j | \mu_{ij} | i \rangle|$  is the transition matrix element of the dipole moment between the  $i$  and  $j$  Zeeman levels,

$\Delta v_{\pm}$  is the Zeeman frequency displacement from the peak of the transition.

$$\Delta v_{\pm} = v - v_0 \mp g\beta B. \quad (46)$$

$v_0$  is the zero field absorption line center,

$g$  is the rotational gyromagnetic ratio of the ground state,

$\beta$  is the Bohr magneton,

$B$  is the magnetic field strength.

ReZ is the real part of the plasma dispersion function,  $Z(\zeta)$ , given by,

$$Z(\zeta) = \frac{1}{\sqrt{\pi}} \int_{-\infty}^{+\infty} \frac{\exp(-t^2)}{t - \zeta} dt. \quad (47)$$

The plasma dispersion function occurs in the propagation of electromagnetic waves through plasma-like media.

$$R_{\Delta}(M_j) = \sum_{M_j} \frac{N_i |<j|\mu_{ij}|i>|^2}{g_i 2uh\epsilon_0} \{ \text{Re}Z[(\Delta v_+ + i\delta)\lambda/u] - \text{Re}Z[(\Delta v_- + i\delta)\lambda/u] \} \quad (48)$$

$$= \frac{N_i |<j|\mu_{ij}|i>|^2}{g_i 2uh\epsilon_0} \{ 2\sqrt{\pi} \exp(\lambda^2 \delta^2 / u^2) [ \exp(-\lambda^2 \Delta v_+^2 / u^2) \sin(2\delta \Delta v_+ \lambda^2 / u^2) - \exp(-\lambda^2 \Delta v_-^2 / u^2) \sin(2\delta \Delta v_- \lambda^2 / u^2) ] \}$$

by complex integration.

### THE SIGNAL-TO-NOISE RATIO OF DETECTION

Steady illumination by a source produces a d.c current which brings with it shot noise.

Shot noise puts a lower limit on the signal level able to be detected.

The shot noise associated with a d.c current I is,

$$I_{\text{shot}} = \sqrt{(2eI\Delta f)}. \quad (49)$$

where  $\Delta f$  is the frequency bandwidth of detection, and e is the electron charge in Coulombs.

Photodetectors produce an electrical current proportional to the incident photon flux by the generation of carriers in a semiconductor, or electron emission from the cathode in a vacuum diode or photomultiplier. These detectors are characterized by a quantum efficiency  $\eta$  which is the ratio of the charged particle current collected at the terminals to the rate of incident photons.

The current  $I_0$  due to an optical power P is,

$$I_0 = \eta e P / h\nu. \quad (50)$$

where  $P/h\nu$  is the rate of photons incident on the detector,  $\nu$  is the frequency of the radiation and e is the electron charge. The quantum efficiency is normally less than unity. If each primary carrier produces secondary carriers, for example by secondary emission in a photomultiplier, the process is taken into account by a gain factor G;

$$I_0 = G\eta e P / h\nu. \quad (51)$$

The signal to noise ratio of detection is defined as the ratio of the mean square signal current  $\overline{I_s}^2$  to the mean square noise current  $\overline{I_n}^2$ .

$$S/N = \overline{I_s}^2 / \overline{I_n}^2. \quad (52)$$

The signal is detectable only when the S/N is  $\geq 1$ . Denoting the power of the incident optical radiation by  $P_I$ , the mean square signal current from the detector is,



$$\overline{I_s} \overline{I^2} = G^2 (e\eta/h\nu)^2 \overline{P_1^2} \quad (53)$$

where  $\eta$  is the quantum efficiency of the photodetector, and  $\nu$  is the frequency of the incident photons, assuming that the detection bandwidth is chosen to be narrow compared to the optical frequency, so that one value of  $\nu$  can be used to describe the incident photons. The mean square noise current is,

$$\overline{I_n} \overline{I^2} = 2eI_0 \Delta f \quad (54)$$

The d.c current  $I_0$  is produced by the signal power. The signal to noise ratio is therefore

$$S/N = G^2 (e\eta/h\nu)^2 \overline{P_1^2} / (2eI_0 \Delta f) \quad (55)$$

The NEP is the value of the root mean square incident power for which the signal to noise ratio is 1. Therefore ,

$$NEP = h\nu / G\eta \sqrt{(2I_0 \Delta f / e)} \quad (56)$$

The NEP is proportional to the area of the detector and the frequency bandwidth of detection. To make the NEP independent of these quantities, a quantity  $D^*$  (detectivity) is defined which is a kind of normalized NEP. With photodetectors it is a characteristic of the noise associated with the generation of primary (and in the case of PMTs, secondary) carriers.

$$D^* = (\sqrt{A \Delta f}) / NEP = (G\eta/h\nu) \sqrt{(eA/2I_0)} \text{ cm Hz}^{1/2} \text{ W}^{-1} \quad (57)$$

The unit of detectivity is the Jones ( $1 \text{ Jones} = 1 \text{ cm Hz}^{1/2} \text{ W}^{-1}$ ) which is defined as the signal to noise ratio to be expected from a 1cm detector in a 1 second integration for a 1 Watt input.

For the detection of free radicals such as OH which absorb strongly in the UV, a photoemissive detector such as the PMT (Photomultiplier tube) is used. These detectors have relatively low noise and are capable of detecting single photons. In a PMT, photoelectrons produced at the photocathode are accelerated through a potential difference and strike a series of secondary emitting surfaces called dynodes which are held at progressively more positive voltages. In this way, electron multiplication is achieved and a sizeable current can be obtained at the anode.

#### DERIVATION OF SIGNAL-TO-NOISE RATIO EXPRESSIONS

The net rate of energy loss in a frequency range  $d\nu$  from a light beam with energy density  $S$  sent through a cell of volume  $V$  containing absorbing molecules is the rate at which energy is removed by absorption minus the rate at which energy is returned by stimulated emission.

$$dE/dt = (N_0 B S h\nu - N_1 B S h\nu) g(\nu - \nu_0) d\nu \quad (58)$$

where

E is the energy,

$g(\nu - \nu_0)d\nu$  is the fraction of transitions for which the frequency of absorbed photons lies in the range  $d\nu$ ,

S is the energy density of the beam in  $J/m^3$ ,

B is the Einstein coefficient for absorption and stimulated emission ( $B_{01} = B_{10} = B$ ),

$N_0$  and  $N_1$  are the number of molecules in the ground and excited states respectively.

Let  $I_0$  = Irradiance incident normal to the cross-sectional area A of the sample cell in  $W/m^2$ ,

$I(z)$  = Irradiance in  $W/m^2$  incident on the detector on a resonance,

z = length of the sample cell in m.

$$dS/dt = -(N_0 - N_1)g(\nu - \nu_0)BSh\nu/V. \quad (59)$$

since  $S = I/c\chi$  where  $\chi$  is the refractive index of the medium. V is the volume of the cell in which the molecules are contained.

$$dI/dz = -(N_0 - N_1)g(\nu - \nu_0)Bh\nu I/Vc\chi. \quad (60)$$

$N_0 - N_1 = \frac{NA_{10}}{A_{10} + 2BS}$  at steady state where N is the total number of molecules.

$$\frac{NA_{10}}{A_{10} + 2BS} = \frac{NA_{10}}{A_{10} + (2BI/c\chi)}. \quad (61)$$

$$\text{so that } (1 + 2BI/A_{10}c\chi)dI/I = -NBh\nu g(\nu - \nu_0)/Vc\chi. \quad (62)$$

For non-laser light sources,  $2BS/A = 2BI/Ac\chi \ll 1$ .

so that  $I(z) = I_0 \exp[(-NBh\nu g(\nu - \nu_0)/Vc\chi)z]$ .

$$= I_0 \exp(-Kz). \quad (63)$$

where K is the absorption coefficient in  $m^{-1}$ .

$$\text{For a monochromatic source, } K = [NBh\nu g(\nu - \nu_0)]\nu = \nu_0/Vc\chi. \quad (64)$$

$$\text{For a broad-band source, } K = \int [NBh\nu g(\nu - \nu_0)d\nu] / (Vc\chi) \int d\nu/\nu, \quad (65)$$

where the integrations are done over the range of frequencies present in the light source.

For a very intense light source such as a laser,  $2BS \gg 1$ .

$$\text{and } I(z) = I_0 - NA_{10}h\nu g(\nu - \nu_0)z/2V. \quad (66)$$

On a resonance, the signal from the detector is due to an intensity  $[I_0 - I(z)]$  absorbed by the molecules in the sample cell and the change in the power incident on the detector with active area

$A_d$  is  $[I_0 - I(z)]A_d$ .

The change in the current output from the detector due to the absorption is  $e\eta[I_0 - I(z)]A_d/h\nu$ .

The signal due to the absorption will be  $\int_{t_1}^{t_2} \{G\eta e[I_0 - I(z)]A_d/h\nu\} f(t - t_0) dt$ .

where  $f(t - t_0)$  is the distribution function of the current pulse from the anode of the PMT. It will be assumed Gaussian.

$$f(t - t_0) = \frac{2(\ln 2)^{1/2}}{\pi^{1/2}\Delta t} \exp[-4\ln 2(t - t_0)^2/\Delta t^2].$$

where

$t_0$  is the transit time between photoemission at the cathode and the appearance of a pulse at the anode,

$\Delta t$  is the transit time spread (width at half maximum) of the pulse from the anode of the PMT, and  $t_2 - t_1$  is the duration of the anode pulse.

The shot noise,  $I^{\text{shot}}$  due to  $I(z)$  is  $G\eta \int_{t_1}^{t_2} [2e^2 I(z) \Delta f A_d / h\nu]^{1/2} f(t - t_0) dt$ .

The thermal detector noise,  $N_t$ , is given by,

$$N_t = 2[4kT_D \Delta f / R]^{1/2}. \quad (67)$$

where  $k$  = Boltzmann's constant ( $1.38066 \times 10^{-23} \text{ JK}^{-1}$ ),

$T_D$  = detector temperature,

$\Delta f$  = detection bandwidth,

$R$  = detector effective resistance.

The shot noise from the detector is equal to  $\sqrt{2eI_n \Delta f}$  where  $I_n$  is the dark current from the detector.

In MRS, the power from a monochromatic source passed through the polarizer after the sample, for a weak line and small uncrossing angle  $\xi$  is,

$$P_T = P_0(1 - \cos 2\xi)/2.$$

The current from the detector due to this power is  $P_T e\eta/h\nu$  or  $e\eta P_0(1 - \cos 2\xi)/2h\nu$  in terms of the power or  $e\eta I_0(1 - \cos 2\xi)A_d/2h\nu$  in terms of the irradiance incident on the sample cell.

The shot noise,  $I_{\text{MRS}}^{\text{shot}}$  due to the transmitted power is then,

$$I_{\text{MRS}}^{\text{shot}} = G\eta \int_{t_1}^{t_2} [e^2 I_0(1 - \cos 2\xi) \Delta f A_d / h\nu]^{1/2} f(t - t_0) dt. \quad (68)$$

Let  $(S/N)_0$  be the S/N achieved after time  $T_0$ .  
The S/N at any time T is,

$$S/N = (T/T_0)^{1/2} (S/N)_0 . \quad (69)$$

Letting  $T_0 = 1$  second,

The signal-to-noise ratio for absorption after a time T is,

$$S/N = T^{1/2} \frac{\int_{t_1}^{t_2} |G\eta e[I_0 - I(z)]A_d/h\nu| |f(t - t_0)| dt}{\bar{I}_{\text{shot}} + 4(kT\Delta f/R)^{1/2} + (2e\bar{I}_n\Delta f)^{1/2}} . \quad (70)$$

The signal-to-noise ratio for MRS after a time T will be,

$$(S/N)_0 = T^{1/2} \frac{\int_{t_1}^{t_2} |G\eta eR_{\Delta}LP_0\sqrt{2\alpha}f(t - t_0)|/h\nu |dt}{\bar{I}_{\text{MRS}}^{\text{shot}} + 4(kT\Delta f/R)^{1/2} + (2e\bar{I}_n\Delta f)^{1/2}} . \quad (71)$$

Assuming that a spectrum is divided into resolution elements, the number of resolution elements in the spectrum of range  $\Delta\bar{\nu}$  recorded at a resolution of  $\delta\bar{\nu}$  is  $(\Delta\bar{\nu}/\delta\bar{\nu})$ .

For a spectrum of range  $\Delta\bar{\nu}$  which takes a time T to be recorded at a resolution  $\delta\bar{\nu}$ , the time spent on a spectral resolution element in a grating spectrograph is equal to  $T/(\Delta\bar{\nu}/\delta\bar{\nu})$  because the spectrum is recorded sequentially.

The time spent on a resolution element in a FT spectrometer is T, the total time of the scan.

$$\text{SNR}_{\text{grating}} = (\Delta\bar{\nu}/\delta\bar{\nu})^{-1/2} (T/T_0)^{1/2} (S/N)_0 . \quad (72)$$

$$\text{SNR}_{\text{FT}} = (T/T_0)^{1/2} (S/N)_0 , \quad (73)$$

when shot noise is small compared to detector noise.

So the signal-to-noise ratio obtainable with a FT instrument is greater than that obtainable with a grating instrument by a factor of  $(\Delta\bar{\nu}/\delta\bar{\nu})^{1/2}$  when the dominant form of noise in an experiment is detector noise.

Referring to the signal-to-noise ratio expression for absorption using a dispersive spectrograph;

$$S/N = T^{1/2} \frac{\int_{t_1}^{t_2} |G\eta e[I_0 - I(z)]A_d/h\nu| |f(t - t_0)| dt}{\bar{I}_{\text{shot}} + 4(kT\Delta f/R)^{1/2} + (2e\bar{I}_n\Delta f)^{1/2}} . \quad (74)$$

and the signal-to-noise ratio for MRS;

$$\frac{\underline{S}}{N} = \frac{T^{1/2} \int_{t_1}^{t_2} |G\eta e R_{\Delta} L P_0 \sqrt{2\alpha} f(t - t_0)| / h\nu dt}{\bar{I}_{MRS}^{\text{shot}} + 4(kT\Delta f/R)^{1/2} + (2e\bar{I}_n\Delta f)^{1/2}} . \quad (75)$$

In a detector noise limited experiment, the FT-absorption signal-to-noise ratio will be,

$$\frac{\underline{S}}{N} = \frac{(\Delta\bar{v}/\delta\bar{v})^{1/2} T^{1/2} \int_{t_1}^{t_2} |G\eta e [I_0 - I(z)] A_d / h\nu| f(t - t_0) dt}{\bar{I}^{\text{shot}} + 4(kT\Delta f/R)^{1/2} + (2e\bar{I}_n\Delta f)^{1/2}} . \quad (76)$$

and the FT-MRS signal-to-noise ratio will be,

$$\frac{\underline{S}}{N} = \frac{(\Delta\bar{v}/\delta\bar{v})^{1/2} T^{1/2} \int_{t_1}^{t_2} |G\eta e R_{\Delta} L P_0 \sqrt{2\alpha} f(t - t_0)| / h\nu dt}{\bar{I}_{MRS}^{\text{shot}} + 4(kT\Delta f/R)^{1/2} + (2e\bar{I}_n\Delta f)^{1/2}} . \quad (77)$$

The signal-to-noise ratio can be improved further by averaging over a number of scans because the signal is coherent and proportional to the number of scans while the noise is random and proportional to the square root of the number of scans, making the signal-to-noise ratio proportional to the square root of the number of scans. However, the improvement in signal-to-noise ratio is limited by the memory capacity of the computer used to process the data from the interferogram. The lower the initial signal-to-noise ratio, the more scans can be averaged before the computer runs out of memory.

#### CALCULATION OF SIGNAL-TO-NOISE RATIOS FOR THE ${}^2\Pi_{1/2}$ , P(3/2) LINE IN THE $A^2\Sigma^+ - X^2\Pi$ TRANSITION OF OH.

These expressions will be evaluated for the  ${}^2\Pi_{1/2}$ , P(3/2) line in the  $A^2\Sigma^+ - X^2\Pi$  transition of the OH radical. The OH radicals can be produced by a microwave discharge at 2450MHz through 0.1 - 0.6 Torr of water vapor in a cylindrical sample cell with 0.05 m end diameter. A 0.05 m diameter f/10 lens is used between the light source (assumed monochromatic) and the sample cell to collimate the light beam.

Sending a 0.05 m diameter beam from a 300W Hg-Xe arc lamp (about 2% of the lamp's total power is obtainable in the UV) through an f/10 lens with a diameter of 0.05 m will give an irradiance of,

$$I_0 = 300(0.02)/4\pi(0.05)^2 = 1.91\text{W/m}^2 .$$

The cross sectional area of the sample cell,  $A_s$  is,

$$A_s = \pi(d/2)^2 = \pi(0.05/2)^2 = 1.96 \times 10^{-3} \text{ m}^2 .$$

For the OH transition at  $32342 \text{ cm}^{-1}$  ,

$$\begin{aligned} \text{the Einstein A coefficient, } A_{10} &= \frac{16\pi^3 \nu^3 |\langle 1|\mu|0\rangle|^2}{3\epsilon_0 hc^3} \\ &= 2.73 \times 10^7 \text{ s}^{-1} . \end{aligned}$$

The Einstein B coefficient ( $B_{10} = B_{01} = B$ ) is,

$$B = (c^3/4h\nu^3)A_{10} = 2.96 \times 10^{20} \text{ m}^3/\text{Js} .$$

$$\tau = 1/A_{10} = 3.66 \times 10^{-8} \text{ s} .$$

$$\Delta\nu_{\text{Lorentz}} = 1/2\pi\tau = 4.35 \times 10^6 \text{ s}^{-1} .$$

$$\begin{aligned} \Delta\nu_{\text{Doppler}} &= 7.2 \times 10^{-7} \nu_0 (T/M)^{1/2} . \\ &= 2.9 \times 10^9 \text{ s}^{-1} . \end{aligned}$$

$\Delta\nu_{\text{Doppler}} \gg \Delta\nu_{\text{Lorentz}}$  , therefore the line is mainly Doppler broadened .

$$\text{so } g(\nu - \nu_0) = \frac{2(\ln 2)^{1/2} \exp[-4\ln 2 (\nu - \nu_0)^2 / \Delta\nu^2]}{\pi \Delta\nu_D}$$

$$\begin{aligned} \text{At } \nu = \nu_0, g(\nu - \nu_0) &= \frac{2(\ln 2)^{1/2}}{\pi^{1/2} \Delta\nu_D} . \\ &= 3.2 \times 10^{-10} \text{ s} . \end{aligned}$$

The calculation of the signal for absorption is straightforward. To calculate the MRS signal,  $R_\Delta$  has to be calculated according to the expression,

$$R_\Delta = \frac{N_i |\langle j|\mu_{ij}|i\rangle|^2}{g_i 2uh\epsilon_0} \{ 2\sqrt{\pi} \exp(\lambda^2 \delta^2 / u^2) [ \exp(-\lambda^2 \Delta\nu_+^2 / u^2) \sin(2\delta \Delta\nu_+ \lambda^2 / u^2) - \exp(-\lambda^2 \Delta\nu_-^2 / u^2) \sin(2\delta \Delta\nu_- \lambda^2 / u^2) ] \} .$$

$$|\langle j|\mu_{ij}|i\rangle|^2 = |\langle j|\mu_x + i\mu_y|i\rangle|^2 = |\langle v'|\mu_z|v\rangle|^2 |\langle J', \Omega', M_J'|\lambda_x + i\lambda_y|J, \Omega, M_J\rangle|^2 . \quad (78)$$

where  $v$  is the vibrational quantum number,  $J$  is the total angular momentum,  $\Omega$  is the projection of  $J$  onto the internuclear axis, and  $M_J$  is the  $J$  projection onto the magnetic field direction.

( $X, Y, Z$ ) is the space (lab) fixed coordinate system and ( $x, y, z$ ) is the molecule fixed coordinate system. It is assumed that the rotational part of the Hamiltonian is separable from the

vibrational-electronic part.

The X and Y components of  $\mu$  are chosen for this calculation because their nonvanishing matrix elements obey the selection rule  $\Delta M_J = \pm 1$ .

$$|\langle v' | \mu_z | v \rangle|^2 = |\langle 1 | \mu | 0 \rangle|^2 = e^2 (h/8\pi^2 m \nu). \quad (79)$$

$$m = (N_{OH}/N_A) \times 1.66 \times 10^{-27} \text{ kg/amu} = 7.73 \times 10^{-30} \text{ kg},$$

where  $N_A$  is Avogadro's number.

$$\nu = 9.7 \times 10^{14} \text{ s}^{-1}.$$

$$|\langle v' | \mu_z | v \rangle|^2 = |\langle 1 | \mu | 0 \rangle|^2 = 2.87 \times 10^{-59} \text{ C}^2 \text{m}^2.$$

From direction cosine matrix element tables,

$$|\langle J', \Omega', M_J' | \lambda_x + i\lambda_y | J, \Omega, M_J \rangle|^2 = \frac{[(J \mp M)(J \mp M - 1)]^{1/2} 2[(J + \Omega)(J - \Omega)]^{1/2}}{4J[(2J + 1)(2J - 1)]^{1/2}}. \quad (80)$$

Summing over all possible values of  $M_J$  for the transition,

$$\begin{aligned} \sum_{M_J} |\langle J', \Omega', M_J' | \lambda_x + i\lambda_y | J, \Omega, M_J \rangle|^2 &= \sum_{M_J} \frac{(J + \Omega)(J - \Omega)}{4(2J + 1)(2J - 1)} + \sum_{M_J} \frac{(J + \Omega)(J - \Omega)M^2}{4J^2(2J + 1)(2J - 1)} \\ &\quad - \sum_{M_J} \frac{(J + \Omega)(J - \Omega)}{4J(2J + 1)(2J - 1)}. \end{aligned} \quad (81)$$

Since

$$\sum_{-J}^{+J} 1 = (2J + 1), \quad (82)$$

$$\sum_{-J}^{+J} M^2 = (2J + 1)J(J + 1)/3, \quad (83)$$

$$\sum_{-J}^{+J} M = 0, \quad (84)$$

$$\sum_{M_J} |\langle J', \Omega', M_J' | \lambda_x + i\lambda_y | J, \Omega, M_J \rangle|^2 = \frac{(J^2 - \Omega^2)[1 + 4/3J]}{4(2J - 1)}. \quad (85)$$

$$\text{For } J = 3/2 \text{ and } \Omega = 1/2, \sum_{M_J} |\langle J', \Omega', M_J' | \lambda_x + i\lambda_y | J, \Omega, M_J \rangle|^2 = 17/36.$$

Using the expression shown earlier,

$$R_{\Delta} = \frac{N_i}{g_i} \frac{|\langle j||\mu_i||j \rangle|^2}{2uh\epsilon_0} \{ 2\sqrt{\pi} \exp(\lambda^2 \delta^2 / u^2) [ \exp(-\lambda^2 \Delta v_+^2 / u^2) \sin(2\delta \Delta v_+ \lambda^2 / u^2) - \exp(-\lambda^2 \Delta v_-^2 / u^2) \sin(2\delta \Delta v_- \lambda^2 / u^2) ] \}$$

where  $\Delta v_{\pm} = v - v_0 \mp g\beta B$ .

with  $v = v_0 = 32342 \text{ cm}^{-1}$ ,  $\beta = 4.59 \times 10^{-5} \text{ cm}^{-1}/\text{Gauss}$ ,  $B = 2700 \text{ Gauss}$  (A typical value of the magnetic field strength in MRS experiments with the OH radical).

$$g = \frac{1}{J(J+1)} \left[ \frac{3/2 + 2(J-1/2)(J+3/2) - 3/2\gamma + 3}{[4(J+1/2)^2 + \gamma(\gamma-4)]^{1/2}} \right]. \quad (86)$$

The upper sign corresponds to the  ${}^2\Pi_{1/2}$  state for a Hund's case (a) molecule..

$\gamma$  is the ratio of the spin-orbit coupling constant to the rotational constant for OH and is equal to -7.547.

Using  $J= 3/2$  gives  $g = 0.46$ .

$$\text{and } \Delta v_+ = -0.032 \text{ cm}^{-1} \\ \Delta v_- = 0.032 \text{ cm}^{-1}.$$

$$\delta = \Delta v_{\text{Lorentz}}/2 = 2.18 \times 10^6 \text{ s}^{-1}.$$

The typical pressure in the sample cell is 0.1 Torr. The number of molecules of water vapor per unit volume can be obtained from the relation

$$N = PN_A/RT. \quad (87)$$

This gives  $3.3 \times 10^{21}$  molecules/ $\text{m}^3$ .

Assuming 5% conversion to OH,  $N_{\text{OH}} = 1.7 \times 10^{20}$  molecules/ $\text{m}^3$ . For the purposes of the calculation, it is assumed that all the molecules are in the  $J = 3/2$ ,  $v = 0$ ,  ${}^2\Pi_{1/2}$  state.

$R_{\Delta}$  is calculated to be  $0.933 \text{ m}^{-1}$  assuming that all the Zeeman sublevels are equally populated and that the frequency spacing between  $\Delta M_J = +1$  and  $\Delta M_J = -1$  centroids for all the allowed transitions between the Zeeman sublevels are equal.

The typical dark current (current from the PMT when there is no directly incident light on it) from a Hamamatsu 1P28 PMT held at a potential difference of -900V is 40 nAmps.

The effective resistance R of the detector is about 4 Ohms.

Using typical values such as  $\alpha = 10^{-6}$  (for  $\alpha = 10^{-6}$ , the optimum uncrossing angle  $\xi_{\text{opt}}$  is  $0.08^\circ$ ),  $\Delta f = 5 \text{ kHz}$ ,  $\eta = 1$ ,  $\Delta \bar{v} = 8000 \text{ cm}^{-1}$ ,  $T = 2 \text{ hrs}$ ,  $\delta \bar{v} = 1 \text{ cm}^{-1}$ ,  $t_0 = 1 \text{ ns}$ ,  $t_2 = 2 \text{ ns}$ ,  $t_1 = 0$  and  $\Delta t = 0.1 \text{ ns}$ , the following values for the noise terms are calculated from the equations above.



$$G\eta \int_{t_1}^{t_2} [e^2 I_0 (1 - \cos 2\xi) \Delta f A_d / h\nu]^{1/2} f(t - t_0) dt = 3.46 \times 10^{-9} \text{ Amps.}$$

$$G\eta \int_{t_1}^{t_2} [2e^2 I(z) \Delta f A_d / h\nu]^{1/2} f(t - t_0) dt = 2.42 \times 10^{-6} \text{ Amps.}$$

$$4(kT_D \Delta f / R)^{1/2} = 9.0 \times 10^{-9} \text{ Amps.}$$

$$(2eI_n \Delta f)^{1/2} = 8.0 \times 10^{-12} \text{ Amps.}$$

The calculated signal corresponds to 1% absorption ( $\{ [I_0 - I(z)] / I_0 \} = 0.01$ ) by the OH molecules.

For a 1 meter spectrograph with a diffraction grating with sides of 5 cm and 10 cm containing 1200 grooves/mm being used in the first order, a resolution  $\delta\bar{\nu}$  of  $1 \text{ cm}^{-1}$  is attainable if the grating is used at an angle given by  $\sin^{-1}(1/2W\delta\bar{\nu}) = \sin^{-1}[1/2(10\text{cm})(1\text{cm}^{-1})] = 3^\circ$ .

The moving mirror of the FTS has to have a maximum path length of only  $(0.6/\delta\bar{\nu}) = 0.6 \text{ cm}$  to achieve this resolution.

The calculated signal-to-noise ratios are shown below,

	Signal-to-noise ratio
Dispersive spectrograph absorption	$1.68 \times 10^3$
MRS with spectrograph	$7.92 \times 10^9$
FT-MRS	$8.67 \times 10^{10}$

As was previously stated, the signal-to-noise ratio can be limited by the memory capacity of the computer used to process the interferometric data, so that the practical signal-to-noise ratios for MRS and FT-MRS might be less than those shown above .

## REFERENCES

1. D. B. Keck and C. D. Hause, "Magnetic rotation spectra of the 1-0 vibration-rotation band of Nitric Oxide," *J. Chem Phys* 33., 3458 1960.
2. G. Litfin, C.R. Pollock, R.F. Curl, Jr and F.K. Tittel, "Sensitivity enhancement of laser absorption spectroscopy by magnetic rotation effect," *J. Chem. Phys* 72., 6602 1980.
3. H. A. Haus, *Waves and fields in optoelectronics*, Prentice Hall, New Jersey, 1984.
4. R. Loudon, *The quantum theory of light*, Oxford University Press, Cambridge, 1973.
5. J. H. Moore, C. C Davies and M. A Coplan, *Building scientific apparatus*, Addison Wesley 1989.
6. R. Beer, *Remote sensing by Fourier transform spectrometry*, Wiley-Interscience, New York, 1992.
7. R. Shankar, *Principles of quantum mechanics*, Plenum Press, New York, 1980.
8. D. A. McQuarrie, *Statistical mechanics*, Harper Collins Publishers Inc, New York, 1976.
9. J. T. Hougen, *The calculation of rotational energy levels and rotational line intensities in Diatomic molecules*, National Bureau of Standards monograph 115, 1970.
10. E. B. Saff and A. D. Snider, *Fundamentals of complex analysis for mathematics, science and engineering*, Prentice Hall, New Jersey, 1976.
11. T. A. Blake, C. Chackerian Jr and J. R. Podolske, "Prognosis for a mid-infrared magnetic rotation spectrometer for the in-situ detection of free radicals," communication.
12. P. R. Griffiths, *Transform techniques in chemistry*, Plenum Press, New York, 1978.
13. M. C. McCarthy, J. C. Bloch and R. W. Field, "Frequency-modulation enhanced magnetic rotation spectroscopy: A sensitive and selective absorption scheme for paramagnetic molecules," *J. Chem. Phys* 100., 6331 1994.
14. R. Nanes and D.W. Robinson, "Magnetic rotation spectra of the  $A^2\Sigma^+ - X^2\Pi_1$  transition of OH and OD," *J. Chem. Phys* 55., 963 1971.